Spectral Methods for the Calculation of Risk Measures for Variable Annuity Guaranteed Benefits

Runhuan Feng
Department of Mathematics
University of Illinois at Urbana-Champaign
rfeng@illinois.edu

Hans W. Volkmer
Department of Mathematical Sciences
University of Wisconsin - Milwaukee
volkmer@uwm.edu

Abstract

Spectral expansion techniques have been extensively exploited for the pricing of exotic options. In this paper, we present novel applications of spectral methods for the quantitative risk management of variable annuity guaranteed benefits such as guaranteed minimum maturity benefits and guaranteed minimum death benefits. The objective is to find efficient and accurate solution methods for the computation of risk measures, which is the key to determining risk-based capital according to regulatory requirements. Our example calculations show that two spectral methods used in this paper are highly efficient and numerically more stable than conventional known methods. Hence these approaches are more suitable for intensive calculations involving death benefits.

Key Words. Variable annuity guaranteed benefit, Asian option, risk measures, value at risk, conditional tail expectation, geometric Brownian motion with affine drift, Sturm-Liouville problem, spectral expansion, Green's function.

1 Introduction

Variable annuities are among the most complex equity-based investment products available in the insurance market. Policyholders are offered a variety of subaccounts, each of which has a distinct investment objective. The financial returns in subaccounts are linked to the performance of the funds in which they invest. Without additional guarantee riders, insurers (variable annuity writers) merely act as the steward of policyholders' investment in much the same relation of fund managers to mutual funds. In particular, the financial risks are effectively transferred to policyholders. However, in the past decade, with the increasingly fierce competition with mutual funds, nearly all annuity writers introduced complex option-like guaranteed benefit riders to attract personal investors wary of the downside risk of fund participation. The riders are developed with various types of minimal benefits to protect the policyholders' investment under adverse economic circumstances. As a result, insurers assume a certain portion of financial risks back from policyholders. Thus, the

accurate and efficient assessment of financial risks embedded in guaranteed benefits is crucial for the maintenance and management of guarantee products.

The current market practice of pricing, reserving and setting risk capital for variable annuities relies primarily on Monte Carlo simulations. There have been extensive studies on the applications of simulation techniques to the valuation of various types of guaranteed benefits. See for example, Bauer et al. (2008), Bacinello et al. (2011), Piscopo and Haberman (2011), etc. However, it is acknowledged in the insurance industry that the costs of simulations can sometimes be prohibitive even with the aid of variance reduction techniques. Insurers are often forced to find a balance between accuracy, expenses and the timeliness of delivery on results. Such issues in the industrial practice are well documented in Farr et al. (2008). There are non-statistical procedures for modeling guaranteed benefits in the literature, such as numerical schemes developed for pricing guaranteed minimum withdrawal benefits in Milevsky and Salisbury (2006), Dai et al. (2008), Chen and Forsyth (2008). However, the existing literature almost exclusively focuses on pricing and hedging. Relatively little is known about risk management using non-statistical methods.

From the broader perspective of financial theory, variable annuities can be viewed as path-dependent derivatives. Although the pricing techniques of exotic options are not new, the complexity of modeling variable annuity guaranteed benefits presents rather unique challenges in many aspects. First, insurance products are generally very long-term in relation to short-lived financial derivatives. Regulatory risk capital requirements are set up to ensure variable annuity writers keep sufficient funds to cover unexpected losses. Due to their long-term nature, the guarantee products require frequent valuations and determinations of risk capital. Numerical procedures for the calculation of risk measures may lead to the issue of error accumulation over long horizon. Second, many intricate guarantee features are intertwined in the products. The combination of multiple exotic option types are often more difficult to model than the stand-alone options. Third, the assessment of longevity risks embedded in variable annuities multiplies the computational effort for valuations and setting risk capital.

A close connection between the payoff of Asian options and insurers' liabilities for variable annuity guaranteed benefits was observed and exploited in Feng and Volkmer (2012). The authors provided explicit solutions to a few key quantities, which lead to analytical calculations of commonly used risk measures such as value-at-risk and conditional tail expectation. The methodologies used in the paper were largely based on the joint distribution of geometric Brownian motion and its integral known from the seminar paper by Yor (1992). Tremendous improvements on accuracy and efficiency were observed in comparison with crude Monte Carlo simulations. However, as pointed out in (Feng and Volkmer, 2012, remarks regarding (3.8)), the methods are much less efficient with small volatility parameters, which can be time-consuming for computations involving death benefits.

In this paper, we present applications of two spectral methods both of which are shown to be more efficient than those in Feng and Volkmer (2012). The advantages of spectral methods in the context of quantitative risk management are multifold.

1. Spectral methods are known to work for a variety of asset pricing models. Their applications in the geometric Brownian motion with affine drift model in this paper can be viewed as a first step that lends itself to more general stochastic models.

2. Spectral methods can be used in various ways to provide both exact evaluation and approximations of risk measures, as we shall demonstrate in this paper. That offers great flexibility in addressing the issue of trade-off between accuracy and efficiency, often faced by practitioners.

3. Spectral methods can work for both pricing and computations of risk measures. These two integral parts of product development are often treated separately in practice and in the actuarial literature. The study of spectral methods may offer some hints on the development of a more holistic approach to the management of variable annuity products.

2 Variable annuity guaranteed benefits

We consider two types of variable annuity riders, namely guaranteed minimum maturity benefits (GMMB) and guaranteed minimum death benefits (GMDB). For simplicity, we do not consider dynamic policyholder behavior relating to fund performance, such as high lapses in periods of low fund values. Although surrender charges are not included explicitly, they can be easily incorporated with rider charges. We introduce the "alphabet soup" for the notation to be used in the models.

- G, the initial guarantee level at policy issue. It is typically a fixed amount under the GMMB rider. The guarantee may also accrue compound interest at the rate of δ up to an advanced age. This is referred to as a roll-up option, often seen with the GMDB rider.

- F_t, the market value of the investment account at $t \geq 0$. F_0 is referred to as the initial purchase payment. For simplicity, we assume that no additional purchase payment or withdrawal is allowed.

- S_t, the market value of the underlying equity fund at t. The asset price process of this fund is defined, on a probability space denoted by $(\Omega, \mathbb{P}, \{\mathcal{F}_t\}_{t\geq 0})$, by a geometric Brownian motion (GBM)

$$S_t = S_0 e^{\mu t + \sigma B_t}, \qquad t > 0, \tag{2.1}$$

  where B is a standard Brownian motion. Simple as it is, this model in fact encompasses more general setups, such as a portfolio of risk-free assets and a risky asset, which is driven by a GBM, or a portfolio of multiple assets, each of which is driven by a GBM and the proportion attributable to each remains constant (known as an automatic rebalancing option).

- m, the annualized rate at which all fees and charges are deducted from the investment account. Contract fees and expenses are typically calculated and accrued on a daily basis. Thus it is reasonable for us to treat all charges as being taken out continuously. The charges allocated

to fund the guarantees are also called margin offset and usually split by benefit. We denote the annualized rate of charges allocated to the GMMB by m_e and that to the GMDB by m_d. Note that the total fee m in general includes overheads and other expenses and hence is larger than the sum of rider changes, i.e. $m > m_e + m_d$.

- T, the target value date (or called maturity date), typically a policy anniversary.
- L_0, the present value of future liabilities, discounted at a constant risk-free force of interest of r per year. The rate reflects the overall yield on assets backing up the liabilities.
- τ_x, the future lifetime of a policyholder of age x at issue. The mortality is assumed to be independent of the performance of investment accounts. We denote by ${}_Tp_x$ the probability that a life aged x survives T years and ${}_Tq_x$ the probability that a life aged x dies within T years.

At the end of each trading day, the account value is marked-to-market according to the performance of funds in which it invests, and mortality and expenses (M&E) fees and rider charges are deducted from the account. Hence, without the effect of investment guarantees, the account value at time t is given by

$$F_t = F_0 \frac{S_t}{S_0} e^{-mt}, \qquad 0 \le t \le T, \tag{2.2}$$

and the margin offset income at time t is given by

$$M_t = m_x F_t, \qquad 0 \le t \le T,$$

where m_x is replaced with m_e for the GMMB or m_d for the GMDB.

The GMMB rider offers the investor at maturity T the greater of a minimum guaranteed amount G and the account value at maturity F_T. The VA writer is liable for the difference, called gross liability, should the former exceeds the latter. In consideration of income generated by the collection of margin offsets $\{M_s, 0 \le s \le T\}$, we can formulate for each contract the present value of the net liability, which is the gross liability net of rider charges, as follows.

$$L_0 := e^{-rT}(G - F_T)_+ I(\tau_x > T) - \int_0^{T \wedge \tau_x} e^{-rs} M_s \, \mathrm{d}s. \tag{2.3}$$

The GMDB rider offers the investor at the time of death the greater of a minimum guaranteed amount and the account value at the time of death. However, in practice, death benefits are not paid immediately due to investigation and administrative handling. We use the curtate future lifetime $\kappa_x^{(n)}$ in years rounded to an accounting period end, say, the upper one n-th of a year.

$$\kappa_x^{(n)} := \frac{1}{n} \lceil n\tau_x \rceil,$$

where $\lceil x \rceil$ is the integer ceiling of x. Suppose the investment account is accumulated and rider charges are deducted up until the end of the one n-th year of the policyholder's death and the

death benefit is payable at the end of the one n-th year. Then the net liability under the GMDB rider is given by

$$L_0^{(n)} = e^{-r\kappa_x^{(n)}}(e^{\delta\kappa_x^{(n)}}G - F_{\kappa_x^{(n)}})_+ I(\kappa_x^{(n)} \le T) - \int_0^{T\wedge\kappa_x^{(n)}} e^{-rs} M_s \,\mathrm{d}s. \tag{2.4}$$

It is worthwhile noting that both net liability models, (2.3) for the GMMB and (2.4) for the GMDB, are based on individual contracts. Both models describe interactions between two sources of uncertainty – (1) *Financial risks*, embedded in the put-option-like guaranteed benefits and asset-based fee income. The origin of financial risks goes back to the random subaccount performance described by $\{F_t, t \ge 0\}$. (2) *Mortality/longevity risk* due to the uncertainty of the timing of payments. The mortality/longevity risk is modeled by a random variable, the policyholder's future lifetime τ_x. In these models, both financial and mortality/longevity risks can interact to cause severe positive net liabilities. In contrast, there are other models in the literature and industrial practice where the mortality risk is diversified and the only source of uncertainty is financial risk. Interested readers are referred to Feng (2014) for a comparison of individual and average models.

Two risk measures are of particular importance for determining risk-based capital for variable annuity as required by the National Association of Insurance Commissioners (NAIC). Specific procedures for implementation can be found in the NAIC's annual publication of forecasting and instructions. The first risk measure is the quantile risk measure, also known as the value-at-risk in the banking industry, for $0 < \alpha < 1$:

$$V_\alpha := \inf\{y : \mathbb{P}[L_0 \le y] \ge \alpha\}.$$

The other is the conditional tail expectation, defined for $0 < \alpha < 1$ by

$$\mathrm{CTE}_\alpha := \mathbb{E}[L_0 | L_0 > V_\alpha].$$

In most cases the net liability L_0 is expected to be negative so that profits are generated for the healthy operation of the business. However, for the purpose of risk management, we are interested only in the severe cases under which the net liabilities turn out to be positive. Readers should be reminded that these cases are considered rare events that incur unexpected large losses. Throughout the paper, we shall denote the probability of non-positive liabilities as $\xi_x := \mathbb{P}[L_0 \le 0]$ where x is replaced with e for the GMMB and d for the GMDB.

Using the independence assumption of mortality and equity dynamics and re-arranging terms, we can easily show (cf. Propositions 3.3 and 3.4 in Feng and Volkmer (2012)) that the quantile risk measure for the GMMB rider is determined implicitly for $\alpha > \xi_e$ by

$$1 - \alpha = {}_Tp_x \mathbb{P}(L_0 > V_\alpha | \tau_x > T) = {}_Tp_x P\left(T, \frac{e^{-rT}G - V_\alpha}{F_0}\right), \tag{2.5}$$

where

$$P(T, w) := \mathbb{P}\left[e^{-rT}\frac{F_T}{F_0} + \int_0^T e^{-rs}\frac{M_s}{F_0}\,\mathrm{d}s < w\right].$$

It is clear from its definition that $P(T,w)$ is an increasing function of w for fixed T. Thus, we can easily determine V_α from (2.5) using a root search algorithm. Similarly, the conditional tail expectation is given by

$$\mathrm{CTE}_\alpha = e^{-rT}G - \frac{{}_Tp_x}{1-\alpha}F_0 Z\left(T, \frac{e^{-rT}G - V_\alpha}{F_0}\right),$$

where

$$Z(T,w) := \mathbb{E}\left[\left\{e^{-rT}\frac{F_T}{F_0} + \int_0^T e^{-rs}\frac{M_s}{F_0}\,\mathrm{d}s\right\} I_{\left\{e^{-rT}\frac{F_T}{F_0} + \int_0^T e^{-rs}\frac{M_s}{F_0}\,\mathrm{d}s < w\right\}}\right].$$

Using the same procedure, we can show that the quantile risk measure V_α with $\alpha > \xi_d$ for the net liability of the GMDB rider is determined implicitly by

$$1-\alpha = \sum_{k=1}^{\lceil nT\rceil} {}_{(k-1)/n}p_x\, {}_{1/n}q_{x+(k-1)/n} P\left(\frac{k}{n}, \frac{e^{-(r-\delta)k/n}G - V_\alpha}{F_0}\right), \tag{2.6}$$

and the conditional tail expectation CTE_α with $\alpha > \xi_d$ is given by

$$\begin{aligned}\mathrm{CTE}_\alpha = &\frac{1}{1-\alpha}\sum_{k=1}^{\lceil nT\rceil} {}_{(k-1)/n}p_x\, {}_{1/n}q_{x+(k-1)/n} \\ &\times\left[e^{-(r-\delta)k/n}P\left(\frac{k}{n}, \frac{e^{-(r-\delta)k/n}G - V_\alpha}{F_0}\right)G - F_0 Z\left(\frac{k}{n}, \frac{e^{-(r-\delta)k/n}G - V_\alpha}{F_0}\right)\right].\end{aligned} \tag{2.7}$$

It is evident that the computation of risk measures hinges on the solutions to P and Z. The first solution method proposed by Feng and Volkmer (2012) utilizes the joint distribution of geometric Brownian motion and its integral. With simplification the expressions for P and Z are given by

$$\begin{aligned}P(T,w) = &\sqrt{\frac{2}{\pi^3\sigma^2 T}}\exp\left(\frac{2\pi^2}{\sigma^2 T} - \frac{\nu^2\sigma^2 T}{8}\right)\int_0^\infty \exp\left(-\frac{2w^2}{\sigma^2 T}\right)\sinh y \sin\left(\frac{4\pi y}{\sigma^2 T}\right) \\ &\times\int_0^{\sqrt{w}} \frac{2\rho^\nu}{1+\rho^2+2\rho\cosh y}\exp\left(-\frac{A(1+\rho^2+2\rho\cosh y)}{2(w-\rho^2)}\right)\mathrm{d}\rho\,\mathrm{d}y,\end{aligned} \tag{2.8}$$

$$\begin{aligned}Z(T,w) = &\sqrt{\frac{2}{\pi^3\sigma^2 T}}\exp\left(\frac{2\pi^2}{\sigma^2 T} - \frac{\nu^2\sigma^2 T}{8}\right)\int_0^\infty \exp\left(-\frac{2y^2}{\sigma^2 T}\right)\sinh y \sin\left(\frac{4\pi y}{\sigma^2 T}\right) \\ &\int_0^{\sqrt{w}}\Big[\frac{2\rho^{\nu+2}}{1+\rho^2+2\rho\cosh y}\exp\left(-\frac{A(1+\rho^2+2\rho\cosh y)}{2(w-\rho^2)}\right) \\ &+A\rho^\nu E_1\left(\frac{A(1+\rho^2+2\rho\cosh y)}{2(w-\rho^2)}\right)\Big]\,\mathrm{d}\rho\,\mathrm{d}y\end{aligned} \tag{2.9}$$

where $\nu = 2(\mu - m - r)/\sigma^2$, $A = 4m_x/\sigma^2$ (m_x should be replaced with m_e in the case of GMMB and m_d in the case of GMDB), and $E_1(z)$ is the exponential integral defined by $E_1(z) = \int_z^\infty e^{-t}/t\,\mathrm{d}t$. This method works well for the GMMB rider with modestly small σ (for example, $\sigma = 0.30$). However, the scheme is very time-consuming for the GMDB rider as numerical integration of oscillating function is repeated at multiple time points in (2.6) and (2.7). The second method is to

use numerical inversion of Laplace transforms such as the Gaver-Stehfest algorithm to find P and Z and their Laplace transforms have the following representations.

$$\begin{aligned}\tilde{P}(s,w) &:= \int_0^\infty e^{-sT} P(T,w)\,\mathrm{d}T \\ &= \frac{4}{\sigma^2}\int_0^{\sqrt{w}}\int_0^{(w-\rho^2)/A} \frac{\rho^{\nu-1}}{u}\exp\left\{-\frac{1}{2u}(1+\rho^2)\right\} I_{2\eta}\left(\frac{\rho}{u}\right)\,\mathrm{d}u\,\mathrm{d}\rho, \qquad (2.10)\\ \tilde{Z}(s,w) &:= \int_0^\infty e^{-sT} Z(T,w)\,\mathrm{d}T \\ &= \frac{4}{\sigma^2}\int_0^{\sqrt{w}}\int_0^{(w-\rho^2)/A} \left(\frac{\rho^{\nu+1}}{u}+A\rho^{\nu-1}\right)\exp\left\{-\frac{1}{2u}(1+\rho^2)\right\} I_{2\eta}\left(\frac{\rho}{u}\right)\,\mathrm{d}u\,\mathrm{d}\rho \qquad (2.11)\end{aligned}$$

where $2\eta = \sqrt{8s/\sigma^2+\nu^2}$, $A = 4m_x/\sigma^2$, and $I_{2\eta}(\cdot)$ is the modified Bessel function of the first kind. Although the second method appears to be much more robust with small time parameter k/n and volatility coefficient σ, it still takes more than half-an-hour for the calculation of each quantile risk measure for the GMDB rider in numerical examples shown in Feng and Volkmer (2012).

In Section 3, we shall propose alternative numerical schemes based on entirely different approaches. The goal is to find more efficient methods that work for as small volatility coefficient as $\sigma = 0.10$, which is about the lower end of the range of values used in practice. Specific parameters for the geometric Brownian motion asset models (also called independent lognormal model) that meet the calibration criteria recommended by the American Academy of Actuaries can be found in Appendix 2 of Gorski and Brown (2005).

3 Spectral methods

Spectral expansion methods were widely used for option pricing in a series of works by Davydov and Linetsky (2003), Linetsky (2004a), Boyarchenko and Levendorskiĭ (2007), Fouque et al. (2011), etc., and their applications to Asian options can be found in Linetsky (2004b). In a separate but related line of development, Donati-Martin et al. (2001) derived an explicit solution to the Laplace transform of the price of Asian option with respect to time parameter using Green's function. Another development of Green's function and spectral expansion for option pricing under the geometric Brownian motion with affine drift appeared in Lewis (1998). In the context of variable annuities, we shall demonstrate that these two methods previously developed by various authors for pricing are well suited for the computation of risk measures. In doing so, we hope to show the intricate connections of the two spectral methods.

3.1 Spectral expansion

We shall make use of the following processes $B^{(\nu)} = \{B_t^{(\nu)}, t \geq 0\}$ and $A^{(\nu)} = \{A_t^{(\nu)}, t \geq 0\}$ where

$$B_t^{(\nu)} := \nu t + B_t, \qquad A_t^{(\nu)} := \int_0^t \exp\{2B_u^{(\nu)}\}\,\mathrm{d}u.$$

The following identity in distribution is obtained in Donati-Martin et al. (2001) with reference to the invariance property of the time reversal of Lévy processes. Interested readers are referred to the duality lemma of Lévy process in (Kyprianou, 2006, Lemma 3.4) for time reversal arguments.

Proposition 3.1. *Let ξ and η be two independent Lévy processes, then for fixed t,*

$$\left(\exp(\xi_t), \exp(\xi_t)\int_0^t \exp(-\xi_s-)\,\mathrm{d}\eta_s\right) \sim \left(\exp(\xi_t), \int_0^t \exp(\xi_s-)\,\mathrm{d}\eta_s\right),$$

where $\sim$ means equality in distribution.

This identity in distribution plays a key role in providing an alternative approach to represent the functions P and Z. Letting $\xi_s = 2B_s^{(\nu)}$ and $\eta_s = s$, we obtain for any fixed $t \geq 0$ and $x_0 \in \mathbb{R}$,

$$\exp\{2B_t^{(\nu)}\}x_0 + A_t^{(\nu)} \sim \exp\left\{2B_t^{(\nu)}\right\}x_0 + \exp\left\{2B_t^{(\nu)}\right\}\int_0^t \exp\left\{-2B_s^{(\nu)}\right\}\,\mathrm{d}s.$$

Define the process $X = \{X_t, t \geq 0\}$ by

$$X_t := \exp\left\{2B_t^{(\nu)}\right\}\left\{x_0 + \int_0^t \exp\left\{-2B_s^{(\nu)}\right\}\,\mathrm{d}s\right\}.$$

This process is known as the geometric Brownian motion with affine drift (cf. Linetsky (2004a)). It is easy to show by the Ito formula that the process X is a diffusion process satisfying the SDE

$$\mathrm{d}X_t = [2(\nu+1)X_t + 1]\,\mathrm{d}t + 2X_t\,\mathrm{d}B_t, \quad X_0 = x_0. \tag{3.1}$$

Therefore, it has an infinitesimal generator with diffusion parameter $a(x) = 2x$ and drift parameter $b(x) = 2(\nu+1)x + 1$ given by

$$\mathcal{G}f(x) := \frac{1}{2}a^2(x)f''(x) + b(x)f'(x) = 2x^2 f''(x) + [2(\nu+1)x+1]f'(x).$$

The diffusion has scale and speed densities:

$$\mathfrak{s}(x) := \exp\left\{-\int \frac{2b(x)}{a(x)}\,\mathrm{d}x\right\} = x^{-\nu-1}\exp\{\frac{1}{2x}\}, \qquad \mathfrak{m}(x) := \frac{2}{a^2(x)\mathfrak{s}(x)} = \frac{1}{2}x^{\nu-1}\exp\{-\frac{1}{2x}\}. \tag{3.2}$$

It is well-known (cf. (Øksendal, 2003, p139, Theorem 8.1)) that for any $F \in C_0^2$, $v(t,x) = \mathbb{E}^x[F(X_t)]$ is a solution to the Kolmogorov backward equation

$$\frac{\partial v}{\partial t} = \frac{1}{2}a^2(x)\frac{\partial^2 v}{\partial x^2} + b(x)\frac{\partial v}{\partial x}, \qquad t, x > 0, \tag{3.3}$$

subject to the initial condition $v(0,x) = F(x)$. We note that

$$\mathbb{E}^x[F(X_t)] = \int_{\mathbb{R}} F(y)\mathfrak{p}(t,x,y)\,\mathrm{d}y, \tag{3.4}$$

where $\mathfrak{p}$, known as the transition density function (w.r.t. the Lebesgue measure), satisfies the Kolmogorov forward equation (cf. (Øksendal, 2003, p168, Exercise 8.3))

$$\frac{\partial}{\partial t}\mathfrak{p}(t,x,y) = \frac{\partial^2}{\partial y^2}(a(y)\mathfrak{p}(t,x,y)) - \frac{\partial}{\partial y}(b(y)\mathfrak{p}(t,x,y)), \qquad \text{for all } x, y > 0.$$

Let $p(t,x,y)$ be the transition density function w.r.t. the speed measure, i.e.

$$\mathfrak{p}(t,x,y) = p(t,x,y)\mathfrak{m}(y).$$

Then it is easy to show that p satisfies the Kolmogorov backward equation (3.3). It is known from (Linetsky, 2004b, (23)) that

$$p(t,x,y) = \int_{\nu^2/2}^{\infty} e^{-\Lambda t}\psi(x,\Lambda)\psi(y,\Lambda)\rho'(\Lambda)\,\mathrm{d}\Lambda, \tag{3.5}$$

where

$$\psi(x,\Lambda) = x^{\kappa}\exp\left(\frac{1}{4x}\right)W_{\kappa,iq}\left(\frac{1}{2x}\right), \qquad q := \frac{1}{2}\sqrt{2\Lambda-\nu^2},$$

W is the Whittaker-W function and the spectral function is given by

$$\rho'(\Lambda) = \frac{1}{\pi^2}\left|\Gamma\left(\frac{\nu}{2}+iq\right)\right|^2\sinh(2\pi q). \tag{3.6}$$

Using the scaling property $\sigma B_T \sim 2B_{\sigma^2 T/4}$, we obtain

$$P(T,w) = \mathbb{P}\left[\exp\{2B^{(\nu)}_{\sigma^2T/4}\} + \frac{4m_x}{\sigma^2}A^{(\nu)}_{\sigma^2T/4} < w\right] = \mathbb{P}^{x_0}[X_t < K], \tag{3.7}$$

where $\mathbb{P}^{x_0}$ is the probability measure under which $\mathbb{P}^{x_0}(X_0 = x_0) = 1$, and

$$t := \frac{\sigma^2 T}{4} > 0, \quad \nu := \frac{2(\mu-m-r)}{\sigma^2}, \quad x_0 := \frac{\sigma^2}{4m_x} > 0, \quad K := x_0 w > 0.$$

In practice, the expected rate of return on the risky asset should be greater than risk-free rate plus rate of fees and charges. Otherwise, there is little incentive for the policyholders to invest in variable annuities. Hence, we only consider $\nu \geq 0$ throughout the paper. Similarly, we have

$$\begin{aligned} Z(T,w) &= \mathbb{E}\left[\left\{\exp\{2B^{(\nu)}_{\sigma^2T/4}\} + \frac{4m_x}{\sigma^2}A^{(\nu)}_{\sigma^2T/4}\right\} I\left(\exp\{2B^{(\nu)}_{\sigma^2T/4}\} + \frac{4m_x}{\sigma^2}A^{(\nu)}_{\sigma^2T/4} < w\right)\right] \\ &= \frac{1}{x_0}\mathbb{E}^{x_0}[X_t I(X_t < K)]. \end{aligned} \tag{3.8}$$

Recall that C_0^2 is a determining class (cf. Problem 4.25 in Karatzas and Shreve (1991)) and hence (3.4) holds true for all measurable functions F. After obtaining the expression for p, we can find explicit solutions to the quantities of interests,

$$P(T,w) = \int_0^K p(t,x_0,y)\mathfrak{m}(y)\,\mathrm{d}y, \tag{3.9}$$

$$Z(T,w) = \frac{1}{x_0}\int_0^K yp(t,x_0,y)\mathfrak{m}(y)\,\mathrm{d}y. \tag{3.10}$$

Using the properties of special functions, we can further simplify the double integrals in (3.9) and (3.10) to single integrals. We shall leave the technical proofs in Appendix A. The Whittaker functions used in these representations are available in most computational software packages, such as Maple and Mathematica, etc. Interested readers are referred to (Olver et al., 2010, Chapter 13) for properties of Whittaker functions. The evaluation of these risk measure can be easily implemented with numerical integration.

Proposition 3.2. *For $\nu > 0, T > 0, w > 0$,*

$$P(T,w) = \frac{x_0}{2\pi^2}\exp\left(-\tfrac{1}{4wx_0}\right) w^{(\nu+1)/2}\exp\left(\tfrac{1}{4x_0}\right)$$
$$\times \int_0^\infty e^{-(\nu^2+p^2)t/2} W_{-\frac{\nu+1}{2},\frac{ip}{2}}\left(\tfrac{1}{2wx_0}\right) W_{\frac{1-\nu}{2},\frac{ip}{2}}\left(\tfrac{1}{2x_0}\right)\left|\Gamma\left(\tfrac{\nu+ip}{2}\right)\right|^2 \sinh(\pi p) p\,\mathrm{d}p, \tag{3.11}$$
$$Z(T,w) = \frac{x_0}{2\pi^2}\exp\left(-\tfrac{1}{4wx_0}\right) w^{(\nu+3)/2}\exp\left(\tfrac{1}{4x_0}\right)$$
$$\times \int_0^\infty e^{-(\nu^2+p^2)t/2}\left[W_{-\frac{\nu+1}{2},\frac{ip}{2}}\left(\tfrac{1}{2wx_0}\right) - W_{-\frac{\nu+3}{2},\frac{ip}{2}}\left(\tfrac{1}{2wx_0}\right)\right] W_{\frac{1-\nu}{2},\frac{ip}{2}}\left(\tfrac{1}{2x_0}\right)\left|\Gamma\left(\tfrac{\nu+ip}{2}\right)\right|^2 \sinh(\pi p) p\,\mathrm{d}p, \tag{3.12}$$

where W is the Whittaker-W function and Γ is the gamma function.

As we shall demonstrate in Section 4, it is not surprising that the evaluation of risk measures by (3.11) and (3.12) can be more efficient that by (2.8), (2.9), (2.10) and (2.11), since we only need to compute single integrals. Moreover, we can further reduce the amount of computation by an approximation. The essence of this approximation is to restrict the underlying process X to a finite range $[0, b]$, in which case the corresponding Sturm-Liouville problem (3.3) with irregular singularity at ∞ is reduced to one with an ordinary point at the boundary b. In the evaluation of (3.9) and (3.10), the transition density in the restricted case simplifies to a sum (A.6) as opposed to an integral (3.5) in the unrestricted case. Further details can be found in Appendix A.

Proposition 3.3. *For $\nu > 0, T > 0, w > 0$ and $b \gg x_0, b \gg wx_0$, $P(T,w)$ can be approximated by*

$$P_b(T,w) = x_0\sum_{n=1}^\infty \exp\left(-\frac{(\nu^2+p_n^2)t}{2}\right)\exp\left(-\tfrac{1}{4wx_0}\right) w^{(\nu+1)/2}\exp\left(\tfrac{1}{4x_0}\right)$$
$$\times W_{-\frac{\nu+1}{2},\frac{ip_n}{2}}\left(\tfrac{1}{2wx_0}\right)\frac{p_n\Gamma(\frac{\nu+ip_n}{2})}{\Gamma(1+ip_n)\xi_n} M_{\frac{1-\nu}{2},\frac{ip_n}{2}}\left(\tfrac{1}{2b}\right) W_{\frac{1-\nu}{2},\frac{ip_n}{2}}\left(\tfrac{1}{2x_0}\right), \tag{3.13}$$

and similarly, $Z(T,w)$ can be approximated by

$$Z_b(T,w) = x_0\sum_{n=1}^\infty \exp\left(-\frac{(\nu^2+p_n^2)t}{2}\right)\exp\left(-\tfrac{1}{4wx_0}\right) w^{(\nu+3)/2}\exp\left(\tfrac{1}{4x_0}\right)$$
$$\times\left[W_{-\frac{\nu+1}{2},\frac{ip_n}{2}}\left(\tfrac{1}{2wx_0}\right) - W_{-\frac{\nu+3}{2},\frac{ip}{2}}\left(\tfrac{1}{2wx_0}\right)\right]\frac{p_n\Gamma(\frac{\nu+ip_n}{2})}{\Gamma(1+ip_n)\xi_n} M_{\frac{1-\nu}{2},\frac{ip_n}{2}}\left(\tfrac{1}{2b}\right) W_{\frac{1-\nu}{2},\frac{ip_n}{2}}\left(\tfrac{1}{2x_0}\right), \tag{3.14}$$

where W and M are the Whittaker-W function and the Whittaker-M function respectively, $0 < p_1 < p_2 < \cdots < p_n < \cdots$ are the positive solutions to

$$W_{(1-\nu)/2,ip/2}\left(\tfrac{1}{2b}\right) = 0, \tag{3.15}$$

and

$$\xi_n := \frac{\partial}{\partial p} W_{(1-\nu)/2,ip/2}\left(\tfrac{1}{2b}\right)\Big|_{p=p_n}. \tag{3.16}$$

Remark 3.1. *The values of p_n can be determined numerically from* (3.15)*. This can be accomplished easily in computational software packages such as Maple. For example, we can use Maple's* `fsolve` *function to determine p_n one by one with initial values p_n^* determined by*

$$p_n^*[\ln(4bp_n^*) - 1] = 2\pi\left(n + \frac{\nu}{4} - \frac{1}{2}\right), \qquad n = 1, 2, 3, \cdots.$$

This approximation equation is obtained in (Linetsky, 2004b, (30)).

Remark 3.2. *Here we provide some upper bounds of the approximation errors of P_b and Z_b.*

$$P(T,w) - P_b(T,w) \le \frac{x_0}{b}e^{2(\nu+1)t} + \frac{1}{2(\nu+1)b}(e^{2(\nu+1)t} - 1);$$
$$Z(T,w) - Z_b(T,w) \le \frac{K}{b}e^{2(\nu+1)t} + \frac{K}{2(\nu+1)bx_0}(e^{2(\nu+1)t} - 1).$$

3.2 Green's function

Alternatively, we can also find solutions to the PDE (3.3) by working out the Laplace transform

$$\tilde{v}(\Lambda, x) := \int_0^\infty e^{\Lambda t} v(t,x)\,\mathrm{d}t, \qquad \Lambda < 0, x > 0.$$

Applying Laplace transforms on both sides of (3.3) yields

$$-\mathcal{G}\tilde{v}(\Lambda,x) - \Lambda\tilde{v}(\Lambda,x) = F(x), \tag{3.17}$$

where the operator $\mathcal{G}$ applies to the function $x \mapsto \tilde{v}(\Lambda, x)$. It is known that if $F \in L^2(\mathfrak{m}, (0,\infty))$ then the solution can be represented in terms of the Green's function, denoted by G.

$$\tilde{v}(\Lambda,x) = \int_0^\infty G(x,y,\Lambda)F(y)\mathfrak{m}(y)\,\mathrm{d}y. \tag{3.18}$$

Note that the corresponding Sturm-Liouville problem (A.1) has the solutions

$$\psi_1(x,\Lambda) = x^\kappa \exp\left(\tfrac{1}{4x}\right) W_{\kappa,\eta}\left(\tfrac{1}{2x}\right),$$
$$\psi_2(x,\Lambda) = x^\kappa \exp\left(\tfrac{1}{4x}\right) M_{\kappa,\eta}\left(\tfrac{1}{2x}\right),$$

where $\eta = \sqrt{\nu^2 - 2\Lambda}/2$. The function $\psi_1(\cdot,\Lambda)$ lies in $L^2(\mathfrak{m},(0,1))$ and $\psi_2(\cdot,\Lambda)$ lies in $L^2(\mathfrak{m},(1,\infty))$. Their Wronskian is

$$\frac{1}{\mathfrak{s}(x)}(\psi_1(x,\Lambda)\psi_2'(x,\Lambda) - \psi_1'(x,\Lambda)\psi_2(x,\Lambda)) = -\frac{1}{2}\frac{\Gamma(1+2\eta)}{\Gamma(\eta-\kappa+\frac{1}{2})}.$$

Therefore, Green's function (Jeanblanc et al., 2009, page 278) corresponding to (3.3) is

$$G(x,y,\Lambda) = 2\frac{\Gamma(\eta-\kappa+\frac{1}{2})}{\Gamma(1+2\eta)}\begin{cases}\psi_1(x,\Lambda)\psi_2(y,\Lambda) & \text{if } x < y;\\ \psi_1(y,\Lambda)\psi_2(x,\Lambda) & \text{if } x \ge y.\end{cases} \tag{3.19}$$

It can be shown that the Green's function exists for $\Lambda < \frac{\nu^2}{2}$, as $\nu \geq 0$ by assumption.

In view of (3.7) and (3.18), we obtain

$$\begin{aligned}\tilde{P}(s,w) &:= \int_0^\infty e^{-sT} P(T,w)\,\mathrm{d}T = \frac{4}{\sigma^2}\int_0^\infty e^{-4st/\sigma^2}\mathbb{P}^{x_0}[X_t < K]\,\mathrm{d}t \\ &= \frac{4}{\sigma^2}\int_0^\infty G\left(x_0, y, -\frac{4s}{\sigma^2}\right) I(y<K)\mathfrak{m}(y)\,\mathrm{d}y. \end{aligned} \tag{3.20}$$

Similarly, it follows from (3.8) and (3.18) that

$$\begin{aligned}\tilde{Z}(s,w) &:= \int_0^\infty e^{-sT} Z(T,w)\,\mathrm{d}T = \frac{4}{x_0\sigma^2}\int_0^\infty e^{-4st/\sigma^2}\mathbb{E}^{x_0}[X_t I(X_t < K)]\,\mathrm{d}t \\ &= \frac{4}{x_0\sigma^2}\int_0^\infty G\left(x_0, y, -\frac{4s}{\sigma^2}\right) yI(y<K)\mathfrak{m}(y)\,\mathrm{d}y. \end{aligned} \tag{3.21}$$

A great advantage of this approach is that the two expressions (3.20) and (3.21) can be further simplified to closed-form solutions, which are clearly superior than (2.10) and (2.11) in terms of numerical implementation.

Proposition 3.4. *Let* $\kappa = (1-\nu)/2$, $2\eta = \sqrt{8s/\sigma^2 + \nu^2}$ *and* $\Lambda = -4s/\sigma^2$. *For* $w \leq 1$,

$$\tilde{P}(s,w) = \frac{4x_0}{\sigma^2}\frac{\Gamma(\eta-\kappa+\frac{1}{2})}{\Gamma(1+2\eta)} w^{1-\kappa}\exp\left\{\frac{1}{4x_0}\left(1-\frac{1}{w}\right)\right\} M_{\kappa,\eta}\left(\frac{1}{2x_0}\right) W_{\kappa-1,\eta}\left(\frac{1}{2x_0 w}\right), \tag{3.22}$$

$$\begin{aligned}\tilde{Z}(s,w) = &\frac{4x_0}{\sigma^2}\frac{\Gamma(\eta-\kappa+\frac{1}{2})}{\Gamma(1+2\eta)} w^{2-\kappa}\exp\left\{\frac{1}{4x_0}\left(1-\frac{1}{w}\right)\right\} M_{\kappa,\eta}\left(\frac{1}{2x_0}\right) \\ &\times\left[W_{\kappa-1,\eta}\left(\frac{1}{2x_0 w}\right) - W_{\kappa-2,\eta}\left(\frac{1}{2x_0 w}\right)\right], \end{aligned} \tag{3.23}$$

and, for $w > 1$,

$$\begin{aligned}\tilde{P}(s,w) = &\frac{1}{s} - \frac{4x_0}{\sigma^2}\frac{\Gamma(\eta-\kappa+\frac{1}{2})}{\Gamma(1+2\eta)}\frac{w^{1-\kappa}}{\eta+\kappa-\frac{1}{2}}\exp\left\{\frac{1}{4x_0}\left(1-\frac{1}{w}\right)\right\} \\ &\times W_{\kappa,\eta}\left(\frac{1}{2x_0}\right) M_{\kappa-1,\eta}\left(\frac{1}{2x_0 w}\right), \end{aligned} \tag{3.24}$$

$$\begin{aligned}\frac{\sigma^2 x_0}{4}\tilde{Z}(s,w) = &\frac{1-\Lambda x_0}{\Lambda(\Lambda+2(\nu+1))} - x_0^2\frac{\Gamma(\eta-\kappa+\frac{1}{2})}{\Gamma(1+2\eta)}\frac{w^{2-\kappa}}{\eta+\kappa-\frac{1}{2}}\exp\left\{\frac{1}{4x_0}\left(1-\frac{1}{w}\right)\right\} \\ &\times W_{\kappa,\eta}\left(\frac{1}{2x_0}\right)\left(\frac{M_{\kappa-2,\eta}\left(\frac{1}{2x_0 w}\right)}{\eta+\kappa-\frac{3}{2}} + M_{\kappa-1,\eta}\left(\frac{1}{2x_0 w}\right)\right). \end{aligned} \tag{3.25}$$

Remark 3.3. *We can actually prove analytically that* (3.22) *and* (3.23) *are equivalent to* (2.10) *and* (2.11). *The detailed proof can be found in the Appendix.*

4 Numerical examples

For variable annuity net liability models (2.3) and (2.4), two computational methods for risk measures were proposed in Feng and Volkmer (2012). Solutions to risk measures were represented

in terms of double integrals as shown in (2.8)-(2.11). Although there were tremendous improvements on both accuracy and efficiency over Monte Carlo simulations for modestly small volatility coefficient σ, the computational algorithms appeared to be very slow for smaller values such as $\sigma = 0.1$, which is at the lower end of the range of volatility parameters used by practitioners. In this section, we test the two methods used in this paper, namely the spectral expansion and the Green's function.

We first checked the accuracy of results from the two spectral methods under the same valuation basis as used in Feng and Volkmer (2012). Consider a variable annuity contract issued to a policyholder of age 65 with GMMB and GMDB riders. The term of the variable annuity contract is 10 years, i.e. $T = 10$. The valuation is based on the geometric Brownian motion model (2.1) with $\mu = 0.09$ and $\sigma = 0.3$ per annum. The discount rate, annualized fees/charges, GMMB/GMDB rider charges are given by $r = 0.04, m = 0.01$, and $m_e = m_d = 0.0035$ per annum respectively. The initial guarantee for both GMMB and GMDB is set at the full refund of initial purchase payment, i.e. $G = F_0$. In addition, under the GMDB rider, the guaranteed level accrues compound interest at a roll-up rate of $\delta = 0.06$ per annum, payable in arrears. The probability model of survivorship is extracted from the period life table for male and calendar year 2010 published by the U.S. Social Security Administration (Bell and Miller, 2005, page 68), which we reiterate in Table 1.

x	${}_1q_x$	k	${}_kp_{65}$	x	${}_1q_x$	k	${}_kp_{65}$
65	0.01753	0	1.00000	71	0.03059	6	0.87275
66	0.01932	1	0.98246	72	0.03343	7	0.84606
67	0.02122	2	0.96348	73	0.03633	8	0.81778
68	0.02323	3	0.94304	74	0.03942	9	0.78807
69	0.02538	4	0.92113	75	0.04299	10	0.75700
70	0.02785	5	0.89775	-	-	-	-

Table 1: Predicted mortality rates of a male at the age of 65

We report the results for quantile risk measures and conditional tail expectations at the 90% level in Table 2. The results are reported in the order of (1) double integrals based on Hartman-Watson density, (2) numerical inversion of double integrals based on Laplace transform of Hartman-Watson density, (3) spectral expansion, and (4) Green's function. The computations using spectral expansion are based on the approximation formulas in Proposition 3.3 with the first 30 terms and $b = 100,000$. The calculations using Green's function are based on formulas of $\tilde{P}$ and $\tilde{Z}$ in Proposition 3.4 and the functions P and Z are then obtained by the well-known Gaver-Stehfest numerical inversion algorithm. As the computational performance depends on software package and computer set-up, the data on running times are only intended to provide ballpark estimates. The Newton-Raphson algorithm was applied to find the quantile risk measure with the first method whereas bisection algorithms were used with other three methods. All iterations terminate once the results converge up to seven digits. The running times for the second method are slightly longer than

those reported in Feng and Volkmer (2012) due to the requirement of a higher level of accuracy. All fifteen digits of the quantile estimates were fed into the computation of conditional tail expectation. The results in Table 2 indicate that both spectral methods (3), (4) perform significantly better than the numerical integration methods (1), (2).

Methods	(1)	(2)	(3)	(4)
$V_{90\%}/F_0$	12.550359%	12.550365%	12.550350%	12.550365%
Initial values	10%	(12%, 14%)	(12%, 14%)	(12%, 14%)
Time (secs)	220.445	301.923	51.579	0.172
$\text{CTE}_{90\%}/F_0$	30.296433%	30.296482%	30.296430%	30.296484%
Time (secs)	112.028	17.109	2.953	0

Table 2: A comparison of four computational methods for the GMMB rider

The improvement on efficiency is even more pronounced in the evaluation of risk measures for the GMDB rider. As the functions P and Z are required to be evaluated at multiple points, approximation errors from the spectral method appear to accumulate drastically. In order to increase the level of accuracy, we include the first 100 terms in the expressions for $P_b(t, w)$ and $Z_b(t, w)$. In this case, the calculations based on (1) is omitted as the method is too slow to deliver results for multiple point evaluation. We report on results of risk measures up to eight significant digits with no rounding in Table 3.

Methods	(2)	(3)	(4)
$V_{90\%}/F_0$	2.135314%	2.135314%	2.135314%
Initial values	(0%, 10%)	(0%, 10%)	(0%, 10%)
Time (secs)	4667.041	1622.044	4.953
$\text{CTE}_{90\%}/F_0$	33.706290%	33.706287%	33.706292%
Time (secs)	717.843	226.875	0.828

Table 3: A comparison of three computational methods for the GMDB rider

In a second example, we provide numerical tests on the performance of spectral methods with considerably smaller volatility coefficient, $\sigma = 0.1$. The rest of the valuation basis is given as follows: $\mu = 0.045, r = 0.02, m = 0.01, T = 10$, and $m_e = m_d = 0.0035$. The initial guaranteed benefits for both GMMB and GMDB are 110% of initial purchase payment, i.e. $G/F_0 = 1.1$. The roll-up rate is set at $\delta = 0$ for the GMDB rider. In Table 4, we present the 90% risk measures for the GMMB and 95% risk measures for the GMDB. (As one can extrapolate from the red solid line in Figure 1 which represents the survival probability of the GMDB net liability, the point corresponding to the 90% quantile risk measure has to be to the left of the vertical axis. Since negative net liabilities are not of interest from the viewpoint of risk management, we compute 95% risk measures instead.) In contrast with the two methods based on numerical integration,

the method based on Green's function appears to be numerically stable as there is no significant increase in computation time when comparing Tables 2, 3, 4. Hence, we conclude that the numerical method based on Green's function is the best approach among the four methods in consideration of their accuracy and efficiency.

	GMMB		GMDB
$V_{90\%}/F_0$	5.246319%	$V_{95\%}/F_0$	7.860722%
Initial values	$(0\%, 10\%)$	Initial values	$(0\%, 10\%)$
Time (secs)	0.015	Time	6.594
$\text{CTE}_{90\%}/F_0$	16.856324%	$\text{CTE}_{95\%}/F_0$	8.399616%
Time (secs)	0.094	Time	0.797

Table 4: Computation of risk measures with $\sigma = 0.1$.

Owing to the efficiency of the Green's function approach, we can even afford the plots of the survival function (tail probability) of the net liabilities. The parameters are set as in the previous example. The red solid line in Figure 1 represents the survival function of the GMDB net liability $\mathbb{P}(L_0^{(1)} > y)$ for $y \geq 0$ whereas the black dashed line corresponds to that of the GMMB net liability $\mathbb{P}(L_0 > y)$ for $y \geq 0$. We remark that the GMDB benefits are only payable to the deceased policyholders whereas the GMMB benefits are only payable to the survivors after the contract matures in 10 years. Given the survivorship prediction in Table 1, the quantiles for the GMMB rider tend to be higher than those for the GMDB as the majority are expected to receive GMMB benefits and only the minority are expected for the GMDB benefits. However, as the roll-up option takes effect, the guaranteed benefits for the GMDB rider will rise significantly at later years. In Figure 2, we plot the corresponding survival functions of the GMMB and GMDB riders, represented by the red solid line and the black dashed line respectively, where the GMDB includes the roll-up at the rate $\delta = 0.02$. In this case, the survival function of the GMDB rider tends to have a heavier tail than that of the GMMB rider.

5 Summary and Future Work

The computation of risk measures for variable annuity guaranteed benefits presents interesting theoretical challenges. Feng and Volkmer (2012) proposed two analytical methods for net liability models of a stand-alone contract, which are essentially based on Yor and coauthors' work on the joint distribution of geometric Brownian motion and its time-integral. While there were tremendous improvements on accuracy and efficiency in comparison with Monte Carlo simulations, computational difficulties were observed for the computation of death benefits with small volatility. In this paper, we managed to address this issue by proposing two spectral methods. While we have proven analytically the equivalence of all four methods, the examples suggest that the Green's function approach is the most efficient for numerical implementation.

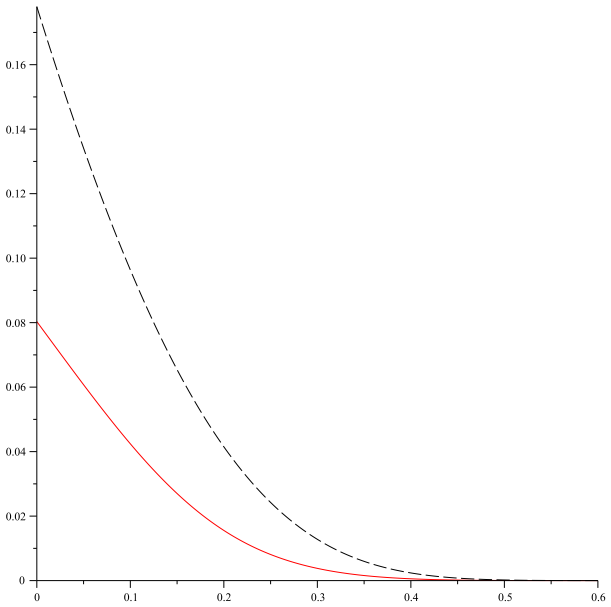

Figure 1: Survival functions of GMMB and GMDB net liabilities with $\delta = 0$

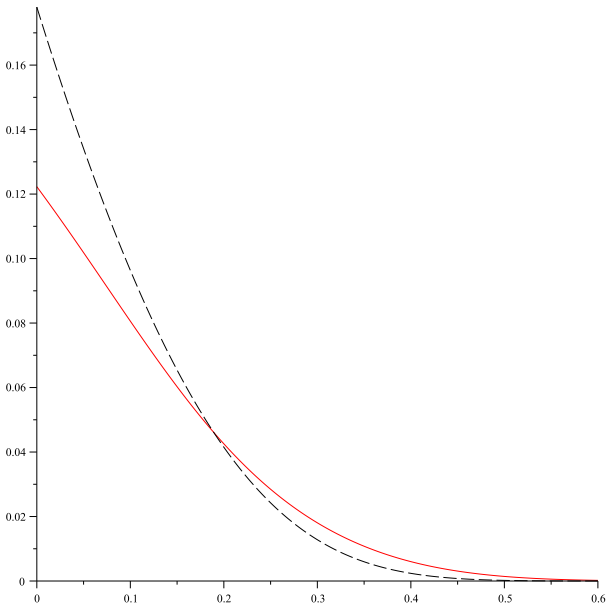

Figure 2: Survival functions of GMMB and GMDB net liabilities with $\delta = 0.02$

Spectral methods are widely studied in the pricing of exotic options. The risk management of equity-linked insurance products appears to be a new territory for theoretical advancement and applications. Although the model considered in this paper has not quite reached the complexity of many GMMB and GMDB products with advanced features, we believe the geometric Brownian motion model offers a good start with valuable insights on the intricate connections among various

analytical techniques. Future research is necessary to build the model on more general processes, such as jump-diffusion or stochastic volatility models, in order to incorporate stylized features of equity prices as well as dynamic policyholder behavior. It is promising that the spectral methods can be further extended for the pricing and risk management of many more advanced variable annuity guaranteed benefits as well. Such an example can be seen in Feng and Volkmer (2013) for the guaranteed minimum withdrawal benefit (GMWB).

A Appendix: Proofs

Proof of Proposition 3.2: Note that $P(T,w) = v(t,x_0)$ which satisfies (3.3) with the initial condition $F(x) = I(x < K)$. Since ψ is a solution to the ODE

$$-2y^2u''(y) - [2(\nu+1)y+1]u'(y) = \Lambda u(y), \qquad y > 0, \tag{A.1}$$

which can be rewritten as

$$-\frac{1}{\Lambda}\left(\frac{\psi'(y,\Lambda)}{\mathfrak{s}(y)}\right)' = \psi(y,\Lambda)\mathfrak{m}(y). \tag{A.2}$$

It immediately follows from (A.2) that

$$c(\Lambda) := \int_0^K \psi(y,\Lambda)\mathfrak{m}(y)\,\mathrm{d}y = -\left.\frac{\psi'(y,\Lambda)}{\Lambda\mathfrak{s}(y)}\right|_0^K.$$

We can show that

$$-\frac{\psi'(y,\Lambda)}{\Lambda\mathfrak{s}(y)} = \frac{1}{2}\exp\left(-\frac{1}{4y}\right)y^{(\nu+1)/2}W_{-(1+\nu)/2,ip/2}\left(\frac{1}{2y}\right).$$

It follows from the asymptotics of the Whittaker function (cf. (Olver et al., 2010, (13.19.3)))

$$-\frac{\psi'(y,\Lambda)}{\Lambda\mathfrak{s}(y)} \sim 2^{1-\kappa}\exp\left(-\frac{1}{2y}\right), \qquad \text{as } y \to 0.$$

Therefore,

$$c(\Lambda) = \frac{1}{2}\exp\left(-\frac{1}{4K}\right)K^{(\nu+1)/2}W_{-(1+\nu)/2,ip/2}\left(\frac{1}{2K}\right). \tag{A.3}$$

We substitute $q = p/2$ and $\Lambda = (\nu^2+p^2)/2$ in (3.9) and hence obtain (3.11).

Similarly, we have $Z(T,w) = v(t,x_0)$ with the initial condition $F(x) = xI(x<K)$. In this case, we use

$$d(\Lambda) := \int_0^K y\psi(y,\Lambda)\mathfrak{m}(y)\,\mathrm{d}y.$$

It is known from Linetsky (Linetsky, 2004b, (43)) that

$$\int_0^K (K-y)\psi(y,\Lambda)\mathfrak{m}(y)\,\mathrm{d}y = \frac{1}{2}K^{(\nu+3)/2}\exp\left(-\frac{1}{4K}\right)W_{-\frac{\nu+3}{2},\frac{ip}{2}}\left(\frac{1}{2K}\right). \tag{A.4}$$

In view of (A.3) and (A.4) we obtain

$$d(\Lambda) = \frac{1}{2}K^{(\nu+3)/2}\exp\left(-\frac{1}{4K}\right)\left[W_{-\frac{\nu+1}{2},\frac{ip}{2}}\left(\frac{1}{2K}\right) - W_{-\frac{\nu+3}{2},\frac{ip}{2}}\left(\frac{1}{2K}\right)\right]. \tag{A.5}$$

Thus we arrive at (3.12) using $\Lambda = (\nu^2 + p^2)/2$ and (A.5) in (3.10). □

Proof of Proposition 3.3: We approximate $P(T, w)$ by

$$P_b(T, w) := \mathbb{P}^{x_0}\left[X_t < K, t < T_b\right],$$

where $T_b := \inf\{t \geq 0 : X_t = b\}$ and $b \gg K$. We denote by $p_b(t; x, y)$ the transition probability density with respect to the speed measure of the diffusion process (3.1) started at $x \in [0, b)$ and killed at b. According to Linetsky (2004b), the transition probability density $p_b(t; x, y)$ is given by

$$p_b(t; x, y) = \sum_{n=1}^{\infty} e^{-\Lambda_n t}\frac{\psi(x, \Lambda_n)\psi(y, \Lambda_n)}{\parallel \psi(\cdot, \Lambda_n) \parallel^2}, \tag{A.6}$$

where $\{\Lambda_n, \psi_n\}_{n=1}^{\infty}$ are eigenvalues and eigenfunctions of the Sturm-Liouville problem

$$-\mathcal{G}u(x) - \Lambda u(x) = 0, \qquad x \in (0, b), \tag{A.7}$$

with the boundary conditions at 0 and b given by

$$\lim_{x\downarrow 0}\frac{u'(x)}{\mathfrak{s}(x)} = 0 \qquad \text{(entrance boundary)}, \tag{A.8}$$

$$u(b) = 0 \qquad \text{(absorption boundary)}. \tag{A.9}$$

Equation (A.7) can also be written as

$$-\frac{1}{\mathfrak{m}(x)}\left(\frac{u'(x)}{\mathfrak{s}(x)}\right)' = \Lambda u(x), \qquad x \in (0, b). \tag{A.10}$$

The eigenfunctions ψ_n form an orthonormal basis in $L^2(\mathfrak{m}, [0, b])$ with the inner product $(f, g) = \int_0^b f(x)g(x)\mathfrak{m}(x)dx$ and the norm $\parallel f \parallel^2 = (f, f)$. For $t > 0$, the spectral representation (A.6) converges uniformly in x, y on $[0, b] \times [0, b]$.

One can show that the solution to (A.7) satisfying the boundary condition (A.8) is given by

$$\psi(x, \Lambda) = x^{(1-\nu)/2}\exp\{\frac{1}{4x}\}W_{\kappa,\mu}\left(\frac{1}{2x}\right).$$

Since the eigenfunction ψ must also satisfy the boundary condition (A.9), we can determine the eigenvalues by finding the zeros of $\psi(b, \Lambda)$. Let $0 < p_1 < p_2 < \cdots < p_n < \cdots$ be the positive solutions to (3.15). The eigenvalues are $\{\Lambda_n = (\nu^2 + p_n^2)/2, n = 1, 2, \cdots\}$. The eigenfunctions are given by

$$\psi(x, \Lambda_n) = x^{(1-\nu)/2}\exp\{\frac{1}{4x}\}W_{(1-\nu)/2,(ip_n)/2}\left(\frac{1}{2x}\right), \qquad n = 1, 2, \cdots. \tag{A.11}$$

The norms of these eigenfunctions are given in (Linetsky, 2004b, (33)) by

$$\frac{1}{\parallel \psi(\cdot,\Lambda_n) \parallel^2} = \frac{2p_n\Gamma((\nu+ip_n)/2)}{\Gamma(1+ip_n)\xi_n} M_{(1-\nu)/2,(ip_n)/2}\left(\frac{1}{2b}\right), \qquad n=1,2,\cdots. \tag{A.12}$$

Therefore, the approximation of $P(T,w)$ is given by

$$P_b(T,w) = \int_0^K p_b(t;x_0,y)\mathfrak{m}(y)\,\mathrm{d}y = \sum_{n=1}^{\infty} e^{-\Lambda_n t}\frac{\psi(x_0,\Lambda_n)}{\parallel \psi(\cdot,\Lambda_n) \parallel^2}\int_0^K \psi(y,\Lambda_n)\mathfrak{m}(y)\,\mathrm{d}y. \tag{A.13}$$

Hence,

$$\begin{aligned}
&P_b(T,V_\alpha)\\
=&\sum_{n=1}^{\infty} 2c_n e^{-(\nu^2+p_n^2)t/2} x_0^{\frac{1-\nu}{2}} e^{\frac{1}{4x_0}} \frac{p_n\Gamma(\frac{\nu+ip_n}{2})}{\Gamma(1+ip_n)\xi_n} M_{(1-\nu)/2,ip_n/2}\left(\frac{1}{2b}\right) W_{(1-\nu)/2,ip_n/2}\left(\frac{1}{2x_0}\right),
\end{aligned}$$

where

$$c_n := \int_0^K \psi(y,\Lambda_n)\mathfrak{m}(y)\,\mathrm{d}y = \frac{1}{2}e^{-1/(4K)}K^{(\nu+1)/2}W_{-(1+\nu)/2,ip_n/2}\left(\frac{1}{2K}\right),$$

using the same arguments as for (A.3). Thus we arrive at the solution (3.13).

Similarly, we can approximate $Z(T,w)$ by

$$Z_b(T,w) := \frac{1}{x_0}\mathbb{E}^{x_0}\left[X_t I_{\{X_t<K, t<T_b\}}\right] = \frac{1}{x_0}\int_0^K y p_b(t;x_0,y)\mathfrak{m}(y)\,\mathrm{d}y.$$

Hence,

$$Z_b(T,V_\alpha) = \frac{1}{x_0}\sum_{n=1}^{\infty} e^{-\Lambda_n t}\frac{\psi(x_0,\Lambda_n)}{\parallel \psi(\cdot,\Lambda_n) \parallel^2} d_n,$$

where as proven in (A.5)

$$d_n = \frac{1}{2}K^{(\nu+3)/2}e^{-1/(4K)}\left[W_{-(\nu+1)/2,ip_n/2}\left(\frac{1}{2K}\right) - W_{-(\nu+3)/2,ip_n/2}\left(\frac{1}{2K}\right)\right].$$

Therefore, we obtain (3.14) after inserting the expression for d_n. □

Proof of Proposition 3.4: Let

$$f_\kappa(y) = y^{-\kappa}\exp\left\{-\frac{1}{4y}\right\}M_{\kappa,\eta}\left(\frac{1}{2y}\right), \qquad g_\kappa(y) = y^{-\kappa}\exp\left\{-\frac{1}{4y}\right\}W_{\kappa,\eta}\left(\frac{1}{2y}\right).$$

It is easy to show that

$$\begin{aligned}
f'_\kappa(y) &= -(\tfrac{1}{2}+\eta+\kappa)f_{\kappa+1}(y), \qquad & g'_\kappa(y) &= g_{\kappa+1}(y),\\
\lim_{y\to 0+} f_\kappa(y) &= 2^\kappa\frac{\Gamma(1+2\eta)}{\Gamma(\eta-\kappa+\frac{1}{2})}, \qquad & \lim_{y\to 0+} g_\kappa(y) &= 0.
\end{aligned}$$

Suppose $w \le 1$ so that $K = wx_0 \le x_0$. In light of (3.19), (3.20), we obtain

$$\begin{aligned}\tilde{P}(s,w) &= \frac{8}{\sigma^2}\frac{\Gamma(\eta-\kappa+\frac{1}{2})}{\Gamma(1+2\eta)}\psi_2\left(x_0,-\frac{4s}{\sigma^2}\right)\int_0^K \psi_1\left(y,-\frac{4s}{\sigma^2}\right)\mathfrak{m}(y)\,\mathrm{d}y \\ &= \frac{4}{\sigma^2}\frac{\Gamma(\eta-\kappa+\frac{1}{2})}{\Gamma(1+2\eta)}\psi_2\left(x_0,-\frac{4s}{\sigma^2}\right)\int_0^K g_\kappa(y)\,\mathrm{d}y \\ &= \frac{4}{\sigma^2}\frac{\Gamma(\eta-\kappa+\frac{1}{2})}{\Gamma(1+2\eta)}\psi_2\left(x_0,-\frac{4s}{\sigma^2}\right)g_{\kappa-1}(K).\end{aligned} \tag{A.14}$$

Inserting the expressions for ψ_2 and g we obtain (3.22).

Similarly, we have

$$\begin{aligned}\tilde{Z}(s,w) &= \frac{8}{x_0\sigma^2}\frac{\Gamma(\eta-\kappa+\frac{1}{2})}{\Gamma(1+2\eta)}\psi_2\left(x_0,-\frac{4s}{\sigma^2}\right)\int_0^K y\psi_1\left(y,-\frac{4s}{\sigma^2}\right)\mathfrak{m}(y)\,\mathrm{d}y \\ &= \frac{4}{x_0\sigma^2}\frac{\Gamma(\eta-\kappa+\frac{1}{2})}{\Gamma(1+2\eta)}\psi_2\left(x_0,-\frac{4s}{\sigma^2}\right)\int_0^K y g_\kappa(y)\,\mathrm{d}y \\ &= \frac{4}{x_0\sigma^2}\frac{\Gamma(\eta-\kappa+\frac{1}{2})}{\Gamma(1+2\eta)}\psi_2\left(x_0,-\frac{4s}{\sigma^2}\right)[Kg_{\kappa-1}(K)-g_{\kappa-2}(K)]\end{aligned} \tag{A.15}$$

which leads to (3.23).

Now suppose $w > 1$ so that $K > x_0$. Splitting the expression for $\tilde{P}$ into two parts, we obtain

$$\begin{aligned}\frac{\sigma^2}{4}\tilde{P}(s,w) &= \int_0^{x_0} G(x,y,-\frac{4s}{\sigma^2})\mathfrak{m}(y)\,\mathrm{d}y + \int_{x_0}^K G(x,y,-\frac{4s}{\sigma^2})\mathfrak{m}(y)\,\mathrm{d}y \\ &= \frac{\Gamma(\eta-\kappa+\frac{1}{2})}{\Gamma(1+2\eta)}x_0\Bigg[M_{\kappa,\eta}\left(\frac{1}{2x_0}\right)W_{\kappa-1,\eta}\left(\frac{1}{2x_0}\right)+\frac{1}{\eta+\kappa-\frac{1}{2}}W_{\kappa,\eta}\left(\frac{1}{2x_0}\right)M_{\kappa-1,\eta}\left(\frac{1}{2x_0}\right) \\ &\quad -\frac{1}{\eta+\kappa-\frac{1}{2}}w^{1-\kappa}\exp\left\{\frac{1}{4x_0}(1-\frac{1}{w})\right\}W_{\kappa,\eta}\left(\frac{1}{2x_0}\right)M_{\kappa-1,\eta}\left(\frac{1}{2x_0w}\right)\Bigg].\end{aligned} \tag{A.16}$$

We simplify this formula using the following observation. If $\kappa > \frac{1}{2}$ then $F(x) = 1$ is in $L^2(\mathfrak{m},(0,\infty))$. Obviously, $\tilde{v}(\Lambda,x) = -\frac{1}{\Lambda}$ is the solution of (3.17) in $L^2(\mathfrak{m},(0,\infty))$. Therefore,

$$-\frac{1}{\Lambda} = \int_0^\infty G(x,y,\Lambda)m(y)\,dy \quad \text{for } x>0. \tag{A.17}$$

Comparing with (A.16) as $w\to\infty$, we find (setting $z=\frac{1}{2x_0}$ and using $-\frac{\Lambda}{2} = (\eta-\kappa+\frac{1}{2})(\eta+\kappa-\frac{1}{2})$)

$$M_{\kappa,\eta}(z)W_{\kappa-1,\eta}(z)+\frac{1}{\eta+\kappa-\frac{1}{2}}M_{\kappa-1,\eta}(z)W_{\kappa,\eta}(z) = \frac{z\Gamma(1+2\eta)}{(\eta+\kappa-\frac{1}{2})\Gamma(\eta-\kappa+\frac{3}{2})}. \tag{A.18}$$

Identity (A.18) holds for all values of κ,η (dropping the assumption $\kappa>\frac{1}{2}$) as we see by inserting the differentiation formulas

$$\begin{aligned}M'_{\kappa,\eta}(z) &= \left(\frac{1}{2}-\frac{\kappa}{z}\right)M_{\kappa,\eta}(z)+\frac{1}{z}(\eta+\kappa+\tfrac{1}{2})M_{\kappa+1,\eta}(z), \\ W'_{\kappa,\eta}(z) &= \left(\frac{1}{2}-\frac{\kappa}{z}\right)W_{\kappa,\eta}(z)-\frac{1}{z}W_{\kappa+1,\eta}(z).\end{aligned}$$

into the Wronskian of Whittaker function,

$$M'_{\kappa,\mu}(z)W_{\kappa,\mu}(z) - M_{\kappa,\mu}(z)W'_{\kappa,\mu}(z) = \frac{\Gamma(1+2\mu)}{\Gamma(1/2+\mu-\kappa)}.$$

Therefore, (A.16) leads to (3.24).

Similarly, we obtain

$$\begin{aligned}\frac{\sigma^2}{4x_0}\tilde{Z}(s,w) = \frac{\Gamma(\eta-\kappa+\frac{1}{2})}{\Gamma(1+2\eta)}\Bigg[& M_{\kappa,\eta}\left(\frac{1}{2x_0}\right)\left(W_{\kappa-1,\eta}\left(\frac{1}{2x_0}\right) - W_{\kappa-2,\eta}\left(\frac{1}{2x_0}\right)\right) \\ & + \frac{1}{\eta+\kappa-\frac{1}{2}} W_{\kappa,\eta}\left(\frac{1}{2x_0}\right)\left(M_{\kappa-1,\eta}\left(\frac{1}{2x_0}\right) + \frac{1}{\eta+\kappa-\frac{3}{2}} M_{\kappa-2,\eta}\left(\frac{1}{2x_0}\right)\right) \\ & - \frac{w^{2-\kappa}}{\eta+\kappa-\frac{1}{2}} \exp\left\{\frac{1}{4x_0}(1-\frac{1}{w})\right\} W_{\kappa,\eta}\left(\frac{1}{2x_0}\right)\left(\frac{M_{\kappa-2,\eta}\left(\frac{1}{2x_0 w}\right)}{\eta+\kappa-\frac{3}{2}} + M_{\kappa-1,\eta}\left(\frac{1}{2x_0 w}\right)\right)\Bigg].\end{aligned} \tag{A.19}$$

We may simplify this formula using the following observation. If $\kappa > 3/2$ then $F(x) = x$ is in $L^2(\mathfrak{m}, (0,\infty))$. Then the corresponding solution of (3.17) is

$$\tilde{v}(\Lambda, x) = \frac{1-\Lambda x}{\Lambda(\Lambda + 2(\nu+1))}.$$

Therefore, we have

$$\frac{1-\Lambda x}{\Lambda(\Lambda+2(\nu+1))} = \int_0^\infty G(x,y,\Lambda) y\, m(y)\, dy \quad \text{for } x > 0. \tag{A.20}$$

By comparing with (A.19) as $w \to \infty$, we obtain (with $z = \frac{1}{2x_0}$)

$$\begin{aligned} & M_{\kappa,\eta}(z)\left(W_{\kappa-1,\eta}(z) - W_{\kappa-2,\eta}(z)\right) + \frac{W_{\kappa,\eta}(z)}{\eta+\kappa-\frac{1}{2}}\left(M_{\kappa-1,\eta}(z) + \frac{M_{\kappa-2,\eta}(z)}{\eta+\kappa-\frac{3}{2}}\right) \\ = & \frac{\Gamma(1+2\eta)}{\Gamma(\eta-\kappa+\frac{3}{2})}\frac{z}{\eta+\kappa-\frac{1}{2}}\left(1 - \frac{2\kappa-2-z}{(\eta-\kappa+\frac{3}{2})(\eta+\kappa-\frac{3}{2})}\right). \end{aligned} \tag{A.21}$$

This identity holds for all κ, η (dropping the assumption $\kappa > 3/2$) as we can see from recursion formulas (Olver et al., 2010, 13.15.1, 13.15.11) for Whittaker functions in combination with (A.18). Now (A.19) and (A.21) lead to (3.25). □

Proof of Remark 3.2: We note that

$$\begin{aligned} P(T,w) - P_b(T,w) &= \mathbb{P}^{x_0}(X_t < K) - \mathbb{P}^{x_0}(X_t < K, t < T_b) = \mathbb{P}^{x_0}(X_t < K, T_b \le t) \\ &\le \mathbb{P}^{x_0}(T_b \le t) = \mathbb{P}^{x_0}\left(\max_{0\le s\le t} X_t \ge b\right). \end{aligned}$$

Since $\nu > 0$ by assumption and X is a submartingale, it follows by Doob's maximal inequality that

$$P(T,w) - P_b(T,w) \le \frac{1}{b}\mathbb{E}^{x_0}[X_t] = \frac{x_0}{b}e^{2(\nu+1)t} + \frac{1}{2(\nu+1)b}(e^{2(\nu+1)t} - 1).$$

Similarly, we note that

$$Z(T,w) - Z_b(T,w) = \frac{1}{x_0}\mathbb{E}^{x_0}[X_t I(X_t < K)] - \frac{1}{x_0}\mathbb{E}^{x_0}[X_t I(X_t < K, t < T_b)]$$
$$\leq \frac{1}{x_0}\mathbb{E}^{x_0}[X_t I(T_b \leq t, X_t < K)] \leq \frac{1}{x_0} K \mathbb{P}^{x_0}\left(\max_{0\leq s\leq t} X_t \geq b\right).$$

□

Proof of Remark 3.3: Here we reiterate the first formula for $\tilde{P}$

$$\tilde{P}_1(s,w) = \frac{4}{\sigma^2}\int_0^{\sqrt{w}}\int_0^{(w-\rho^2)x_0} \frac{\rho^{\nu-1}}{u}\exp\left\{-\frac{1}{2u}(1+\rho^2)\right\} I_{2\eta}\left(\frac{\rho}{u}\right)\,\mathrm{d}u\,\mathrm{d}\rho. \tag{A.22}$$

According to (A.14), the second formula for $\tilde{P}$ is equivalent to

$$\tilde{P}_2(s,w) = \frac{4}{\sigma^2}\frac{\Gamma(\eta-\kappa+\frac{1}{2})}{\Gamma(1+2\eta)} x_0^{\kappa}\exp\left\{\frac{1}{4x_0}\right\} M_{\kappa,\eta}\left(\frac{1}{2x_0}\right)\int_0^{x_0 w} y^{-\kappa}\exp\left\{-\frac{1}{4y}\right\} W_{\kappa,\eta}\left(\frac{1}{2y}\right)\,\mathrm{d}y.$$

In (A.22) we make the substitution

$$u = \frac{2y}{\cosh v + 1}, \quad \rho = \sqrt{\frac{y}{x_0}}\frac{\cosh v - 1}{\sinh v} = \sqrt{\frac{y}{x_0}}\tanh\frac{v}{2}. \tag{A.23}$$

The new variables of integration are v and y. The corresponding limits for these variables are $0 < v < \infty$ and $0 < y < wx_0$. The Jacobian is

$$\sqrt{\frac{y}{x_0}}\frac{1}{\cosh v + 1}.$$

Note that

$$\frac{1}{2u}(1+\rho^2) = \frac{1}{4x_0}(\cosh v - 1) + \frac{1}{4y}(\cosh v + 1), \quad \frac{\rho}{u} = \frac{\sinh v}{2\sqrt{x_0 y}}.$$

After performing the substitution and simplifying we obtain

$$\frac{\sigma^2}{4}\tilde{P}_1(s,w) = \frac{1}{2}\int_0^{x_0 w} x_0^{\kappa-\frac{1}{2}} e^{\frac{1}{4x_0}} y^{-\kappa-\frac{1}{2}} e^{-\frac{1}{4y}} \int_0^{\infty} \exp\left(-\left(\tfrac{1}{4x_0}+\tfrac{1}{4y}\right)\cosh v\right)\coth^{2\kappa}\tfrac{v}{2} I_{2\eta}(\tfrac{\sinh v}{2\sqrt{x_0 y}})\,\mathrm{d}v\,\mathrm{d}y. \tag{A.24}$$

We now use formula (56) in (Buchholz, 1953, page 86):

$$M_{\kappa,\eta}(a_1)W_{\kappa,\eta}(a_2) = \sqrt{a_1 a_2}\frac{\Gamma(1+2\eta)}{\Gamma(\eta-\kappa+\frac{1}{2})}\int_0^{\infty}\exp(-\tfrac{a_1+a_2}{2}\cosh v)\coth^{2\kappa}\tfrac{v}{2} I_{2\eta}(\sqrt{a_1 a_2}\sinh v)\,\mathrm{d}v \tag{A.25}$$

provided that $0 < a_1 < a_2$. We apply (A.25) with $a_1 = 1/(2x_0)$, $a_2 = 1/(2y)$ in (A.24), and we obtain $\tilde{P}_1 = \tilde{P}_2$.

Using the transformation (A.23), we also verify that (3.23) and (2.11) agree. We note that the identity

$$\tanh^2\frac{v}{2} = 1 - \frac{2}{\cosh v + 1}$$

implies $\rho^2 x_0 = y - u$ and thus

$$\frac{\rho^{\nu+1}}{u} + \frac{\rho^{\nu-1}}{x_0} = \frac{\rho^{\nu-1}}{u}\frac{y}{x_0}.$$

Then we argue as above to show that (2.11) transforms to (A.15). □

References

Bacinello, A. R., Millossovich, P., Olivieri, A., and Pitacco, E. (2011). Variable annuities: a unifying valuation approach. *Insurance Math. Econom.*, 49(3):285–297.

Bauer, D., Kling, A., and Russ, J. (2008). A universal pricing framework for guaranteed minimum benefits in variable annuities. *Astin Bull.*, 38(2):621–651.

Bell, F. and Miller, M. (2005). *Life Tables for the United States Social Security Area*. Social Security Administration Publications No. 11-11536.

Boyarchenko, N. and Levendorskiĭ, S. (2007). The eigenfunction expansion method in multi-factor quadratic term structure models. *Math. Finance*, 17(4):503–539.

Buchholz, H. (1953). *Die konfluente hypergeometrische Funktion mit besonderer Berücksichtigung ihrer Anwendungen*. Ergebnisse der angewandten Mathematik. Bd. 2. Springer-Verlag, Berlin.

Chen, Z. and Forsyth, P. A. (2008). A numerical scheme for the impulse control formulation for pricing variable annuities with a guaranteed minimum withdrawal benefit (GMWB). *Numer. Math.*, 109(4):535–569.

Dai, M., Kwok, Y. K., and Zong, J. (2008). Guaranteed minimum withdrawal benefit in variable annuities. *Math. Finance*, 18(4):595–611.

Davydov, D. and Linetsky, V. (2003). Pricing options on scalar diffusions: an eigenfunction expansion approach. *Oper. Res.*, 51(2):185–209.

Donati-Martin, C., Ghomrasni, R., and Yor, M. (2001). On certain Markov processes attached to exponential functionals of Brownian motion; application to Asian options. *Rev. Mat. Iberoamericana*, 17(1):179–193.

Farr, I., Mueller, H., Scanlon, M., and Stronkhorst, S. (2008). *Economic Capital for Life Insurance Companies*. SOA Monograph.

Feng, R. (2014). A comparative study of risk measures for guaranteed minimum maturity benefits by a PDE method. *North American Actuarial Journal*, 18 (4), to appear.

Feng, R. and Volkmer, H. (2012). Analytical calculation of risk measures for variable annuity guaranteed benefits. *Insurance Math. Econom.*, 51(3):636–648.

Feng, R. and Volkmer, H. (2013). An identity of hitting times and its application to the valuation of guaranteed minimum withdrawal benefit. *Preprint*.

Fouque, J.-P., Jaimungal, S., and Lorig, M. J. (2011). Spectral decomposition of option prices in fast mean-reverting stochastic volatility models. *SIAM J. Financial Math.*, 2:665–691.

Gorski, L. M. and Brown, R. A. (2005). Recommended approach for setting regulatory risk-based capital requirements for variable annuities and similar products. Technical report, American Academy of Actuaries Life Capital Adequacy Subcommittee, Boston.

Jeanblanc, M., Yor, M., and Chesney, M. (2009). *Mathematical methods for financial markets*. Springer Finance. Springer-Verlag London Ltd., London.

Karatzas, I. and Shreve, S. E. (1991). *Brownian motion and stochastic calculus*, volume 113 of *Graduate Texts in Mathematics*. Springer-Verlag, New York, second edition.

Kyprianou, A. E. (2006). *Introductory lectures on fluctuations of Lévy processes with applications*. Universitext. Springer-Verlag, Berlin.

Lewis, A. L. (1998). Applications of eigenfunction expansions in continuous-time finance. *Math. Finance*, 8(4):349–383.

Linetsky, V. (2004a). The spectral decomposition of the option value. *Int. J. Theor. Appl. Finance*, 7(3):337–384.

Linetsky, V. (2004b). Spectral expansions for Asian (average price) options. *Oper. Res.*, 52(6):856–867.

Milevsky, M. A. and Salisbury, T. S. (2006). Financial valuation of guaranteed minimum withdrawal benefits. *Insurance Math. Econom.*, 38(1):21–38.

Øksendal, B. (2003). *Stochastic differential equations*. Universitext. Springer-Verlag, Berlin, sixth edition. An introduction with applications.

Olver, F. W. J., Lozier, D. W., Boisvert, R. F., and Clark, C. W., editors (2010). *NIST handbook of mathematical functions*. U.S. Department of Commerce National Institute of Standards and Technology, Washington, DC.

Piscopo, G. and Haberman, S. (2011). The valuation of guaranteed lifelong withdrawal benefit options in variable annuity contracts and the impact of mortality risk. *N. Am. Actuar. J.*, 15(1):59–76.

Yor, M. (1992). On some exponential functionals of Brownian motion. *Adv. in Appl. Probab.*, 24(3):509–531.